Ultrafast plasmonic and real-time label-free polymerase chain reaction

P.Mohammadyousef[a], M.Paliouras[b], M.Trifiro[b], A.G.Kirk[a]
[a]Electrical and Computer Engineering Dept., McGill University, 3480 Rue University, Montréal, QC, H3A 2K6, Canada; [b]Lady Davis Inst. for Medical Research, Jewish General Hospital, 3755 Chemin de la Côte-Sainte-Catherine, Montréal, QC, H3T 1E2, Canada

ABSTRACT

There is a growing focus to adapt Polymerase Chain Reaction (PCR) to point-of-care (POC) testing to provide for a low-cost, rapid and reliable diagnostic instrument. Many studies proposed the integration of microfluidics with fluorophore-assisted or electrochemical amplicon detection methods to introduce a real-time miniature device for POC applications. However, their practicality in POC testing is limited due to their complex microfabrication, high cost, and intrinsic challenges due to their intercalation and hybridization-based detection. In this paper, we present a purely optical methodology without the addition of non-PCR reagents (electroactive or fluorogenic DNA intercalators) to enhance the reliability in quantitative PCR measurement of DNA yield. The determination of PCR results and DNA amplicon quantification are realized by monitoring transmitted power of a 260nm LED in PCR reaction at every thermal cycle. The least-square fits to transmission data demonstrate distinctive features to classify positive vs. negative PCRs and to quantify amplified products. This real-time UV monitoring system was combined with a VCSEL-based plasmonic thermocycler to accomplish fast amplification and detection in a simple and small-scaled footprint applicable for POC diagnostics.

Keywords: Polymerase chain reaction (PCR), point of care (POC), DNA, localized surface plasmon resonance (LSPR), gold nanorods (AuNRs), surface-emitting laser, Threshold cycle, nucleic acids, real-time detection

1. INTRODUCTION

Polymerase Chain Reaction (PCR), invented by Mullis in 1985, revolutionized molecular genetics, and has become a powerful and rapid technique in modern biological and medical sciences for applications such as, cloning, gene expression studies, forensic analysis, and pathogen detection [1-3]. PCR relies on an enzymatic reaction allowing the amplification of a minute number of starting templates. Its specificity and sensitivity originate in enzyme-based amplification of deoxyribonucleic acid (DNA) and sequence-specific hybridizations of short complementary oligonucleotides or "primers" to the target DNA. Normally, a PCR program consists of 30 to 40 repeated temperature cycles carried out in a device referred to as a thermocycler. Each PCR cycle goes through three stages: denaturation of DNA duplexes, primer hybridization, and extension of annealed primers by a heat-stable polymerase. The real-time quantification of amplified target sequence is achieved by combining the thermocycler with a fluorometer in which fluorescence signal is acquired from a fluorescent dye or probe at each thermal cycle. The intensity of the fluorescence signal is plotted versus cycles (amplification plot) and then correlated to the quantity of generated amplicons. A typical amplification plot has a sigmoidal-shaped curve and displays four phases of PCR kinetics: baseline, exponential, linear, and plateau phase. The baseline or background phase is where the florescence signal is below the detection threshold, and it increases exponentially in the most efficient phase (exponential phase) with doubling the amount of amplicons at each cycle if the PCR efficiency is optimal [4]. In linear phase, the amplification rate slows down to enter the plateau phase where amplification ceases due to exhaustion of reagents, thermal inactivation of the DNA polymerase, and inhibitory effect of increased pyrophosphate concentration on polymerase activity [5]. The quantification of amplicons involves determining the crossing point (threshold cycle) at which the fluorescence signal proceeds from the baseline to the exponential phase. The threshold cycle (C_t) is linearly inversely proportional to the logarithm of initial DNA concentration, i.e., for higher starting DNA copy numbers the fluorescent signal enters the exponential phase at earlier cycles. Contrary to end point PCR (gel electrophoresis and digital PCR) in which the final concentration of amplicons in plateau phase is analyzed, qPCR enables relative quantification of initial concentration of a target by comparing C_t values of the target sequence with a sample of known quantity or copy number [6]. Depending on the required level of specificity in PCR, different fluorescent formats are utilized such as intercalating dyes, single-labeled probes (light-up probes) and dual-labeled probes (FRET probes, molecular beacons, scorpion primers). DNA-binding fluorophores are cost-effective, but they are less favorable than oligonucleotide probes due to their potential contamination to PCR products and false positive generation as a result

of binding to primer dimers. Double-labeled probes with PCR blockers (usually hexethylene glycol moiety) provide the most reliable results with no fluorescence emission from nonspecific amplification. However, they need careful probe design to optimize their unfolding (molecular beacons and scorpion primers) and probe hybridization properties; therefore, they are more expensive than intercalating dyes [7].

The functionality of real-time PCR varies depending on the number of different target nucleic acids that can be amplified and analyzed, the method of detection, and the integrated thermocycler. Duplex and multiplex thermocyclers amplify and detect two or more targets in a single PCR experiment by using multiple optical filters for different fluorophores. LightCycler® 480 Instrument II and QuantStudio 5 real-time PCR System manufactured by Roche Diagnostic and Applied Biosystem are equipped with 5 to 6 detection filters. The LightCycler and QuantStudio's thermocyclers are Peltier-based heating/cooling and complete amplification and detection of 348 samples of 5µL and 0.1mL volumes in about 40 and 30 minutes, respectively. However, these real-time thermocyclers suffer from their bulky size (approximately 55 kg), long amplification time, and high-power requirement which makes them a central lab-based and stationary PCR instrument.

Real-time detection methods are categorized into optical and electrochemical groups. The first real-time detection method was fluorescent PCRs, and their integration with microfluidics introduced small-scaled quantitative diagnostic tool for POC applications. Real-time microfluidics offer sub-minute amplification/detection assembled in a low-powered and handheld device by miniaturizing the sample size [8]. Many researchers achieved faster amplification and detection by reducing sample volume to nanoliters scale, and to date Liu et al. used the smallest PCR reaction volume of 3nL amplified in a 20-matrix chip [9]. However, sample miniaturization compromises the sensitivity in detection due to the reduced optical path length through the PCR reaction and necessitates complicated and costly fabrication of microchips and micropipette [10]. Also, the high surface-to-volume ratios in microfluidics causes non-specific adsorption to microchannels which increases noise in fluorescence signal [11]. An optical method other than fluorescent PCR was studied by Roche et al [12]. The absorption of 650nm photodiode laser radiation by suspended 808nm-gold nanorods (AuNRS) in the PCR solution was monitored. The 650nm transmission had no observable change for samples with no DNA polymerase; however, the transmission declined significantly during elongation periods for a positive control with the addition of polymerase. This phenomenon was related to the redshift in AuNRs' absorption spectrum as a result of change in refractive index of their surrounding medium due to amplicon generation. One shortcoming to this inference is that 650nm transmission of different negative controls with the presence of DNA polymerase was not studied to reveal whether the decreasing transmission in positive PCR is due to the polymerase and AuNRs surface interaction or to amplicon generation.

Electrochemistry-based detection of amplicons has been the focus of researchers as an alternative method for optical detection. As a case in point, Fang et al. used methylene blue (MB) as an electroactive DNA intercalator due to its high affinity to guanine bases [13]. During DNA amplification, the population of free MB molecules decreases, which results in a lower current signal measured by bare electrodes. Their detection system was integrated into a microfluidic flow-through device to meet the requirements of a POC instrument. One concern with electrochemical methods is that factors such as temperature, pH, and ionic concentration change as well as accumulation of PCR by-products near the electrodes degrade the sensitivity in detection [11].

In this paper, we benefited from our previously proposed miniaturized photonic thermocycler in which the photothermal heating of evenly dispersed AuNRs in PCR reaction is accomplished by an 808nm vertical-cavity surface emitting laser (VCSEL) irradiation [14, 15]. The thermal energy released from these nanoheaters (excited AuNRs) to PCR solution resulted in a sub-ten-minute amplification for 30 PCR cycles. Our VCSEL-based plasmonic thermocycler was later combined with a novel real-time detection method. The quantification of amplicons and determination of a success (amplification) and fail (no amplification) are accomplished by monitoring UV absorption of free nucleotides (dNTPs) in PCR reaction at every cycle. As the PCR proceeds during elongation stage of every cycle, growing number of dNTPs are incorporated into the newly built DNA strands by polymerase. Once the dNTPs are consumed to form part of the complementary single stranded DNAs (ssDNAs), the delocalized electrons in their heterocyclic rings are less available to interact with photons due to stacking interaction between dNTPs' bases [16]. This results in less UV absorption by bound dNTPs. The unavailability of electrons will be further intensified when bases on ssDNA chain are paired with their complementary bases to form a new double stranded DNA (dsDNA). This structure dependency of UV absorption (hyperchromicity) allows us to monitor the consumption of dNTPs for generated amplicons in PCR. To fulfil this, a 260nm LED was used to irradiate the PCR reaction, and the transmitted optical power was measured using a 150-550nm gain amplified photodetector. The optical power was plotted against cycles (amplification curve) to analyze the behaviour of UV transmission. The amplification curves exhibit a monotonically increasing exponential curve (fail) or a combination of exponential and sigmoid curve (success) intersecting at C_t. The curve shapes serve as a fingerprint to differentiate

successful and failed PCRs, and C_t values are used for absolute quantification of DNA concentration. The absence of fluorogenic probes and fully relying on optical measurements of one PCR ingredient eliminate false positive incidents due to "misprimed" amplification products, primer dimers, and degraded quencher molecule existing in fluorescent PCR. Also, maintaining the conventional sample volume of 20µL further enhance the sensitivity and reliability in detection. This proposed real time PCR system would be ideal for POC applications due to its fast amplification, label-free quantification, simple and small configuration, and large reaction volume which leads to more convenience in fluid handling for on-site sample analysis.

2. EXPERIMENTAL

2.1 PCR sample preparation

20µL PCR reaction was prepared using HemoKlentaq polymerase and its buffer purchased from New England Biolabs (Ipswich, MA). 5µM of forward and reverse primers with sequences of 5'-TCCGGAGCGAGTTACGAAGA-3' and 5'-AATCAATGCCCGGGATTGGT-3' were used for 10^5 copies of *Chlamydia Trachomatis* Strain LGV III (ATCC, Manassas, VA). Poly(enthylene glycol)-modified gold nanorods (PEG-AuNRs) purchased from Nanopartz (Loveland, CO) with 50nM concentration were suspended with the rest of the ingredients in 0.2ml thin walled PCR tube. The AuNRs' plasmon absorption peaks are at 507 and 808nm. The volume of ingredients is based on the PCR guideline provided in polymerase's datasheet. The only modification is that 1µL (or 2.5nM) of PEG-AuNRs was added while the volume of double distilled water (ddH_2O) was decreased. The reaction was capped with 50µL mineral oil.

2.2 Instrument Design

The main components of plasmonic thermocycler are the VCSEL, fan, and Infrared (IR) thermometer. The 808nm 2W VCSEL (Tyson Technology Co., Shenzhen, China) is placed 3mm below the PCR tube, and active cooling is carried out by placing a 14V DC brushless fan on top of tube. An IR thermometer (Optris GmbH, Berlin, Germany) measures the tube's surface temperature. The PWM pin of the VCSEL's driver is connected to an Arduino microcontroller to vary the current going through the VCSEL and as a result the VCSEL's optical power. The gate-source input voltage of a MOSFET switch (V_{GS}) is biased by Arduino to regulate the fan.

The real-time UV monitoring consists of a 1mW 260nm LED, photodetector, and two UV-AR coated plano-convex (PCX) lenses of 6mm EFL (Edmund Optics) (**Figure 1**). The UV LED and photodetector were purchased from Thorlabs. The LED has maximum wavelength at 260nm (±5nm) and optical output power of 1mW at 100mA. A constant current source (STCS2A) purchased from STMicroelectronics feeds the UV LED with 100mA, and its optical power is regulated via the PWM pin of UV LED's driver connected to Arduino. The photodetector's wavelength range is between 150 to 550nm with its peak wavelength at 440nm and maximum responsivity of 0.12A/W. The photodetector's signal goes through a 16-bit ADC to improve Arduino resolution and measurement accuracy, and then connected to Arduino's I2C pins. The positions of optical components (PCX lenses) with respect to PCR tube are calculated using ZEMAX non-sequential mode, an optical design program, to optimize optical path length for maximum UV LED's power at photodetector sight. The UV LED is modeled based on its fair-field intensity distribution provided in its datasheet. In our design, the photodetector image in **Figure 1.b** demonstrates that with 35mm optical path length and properly positioning the PCX lenses, 40% of UV LED power arrives at photodetector.

(a)

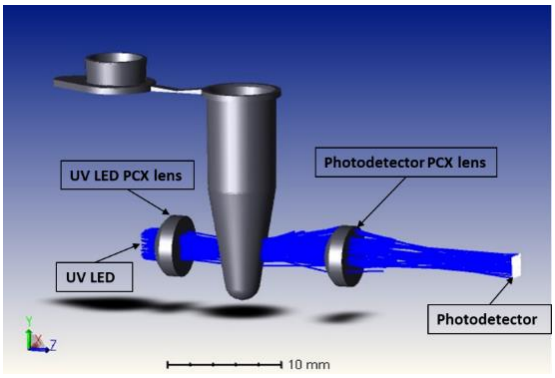

(b)

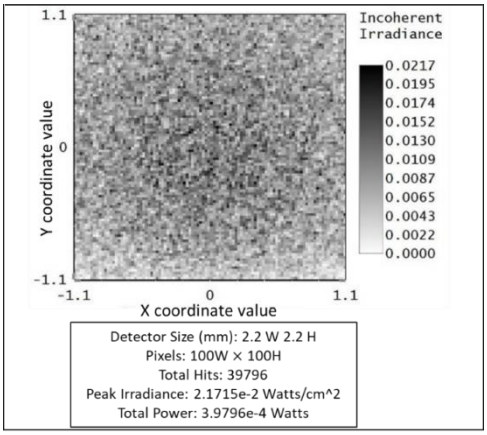

Figure 1. (**a**) 3D layout of 2 lens UV monitoring system and (**b**) Irradiance view at photodetector.

2.3 Working principle

The detailed explanation of the plasmonic amplification was outlined in our previous work [14]. AuNRs are irradiated by an 808nm 2W VCSEL at their resonance wavelength. The non-radiative decay of localized surface plasmons causes local heat generation. Due to high conductivity and relaxation time of AuNRs in a picosecond time scale, the heat is transferred to PCR solution rapidly via convection [17, 18]. The photothermal heating continues to reach denaturation temperature (T_D=85°C), and the temperature is kept constant at T_D for 1s. The V_{GS} of fan's MOSFET switch is biased more than its threshold voltage by one of digital pins of Arduino, and active cooling lowers the temperature to reach annealing temperature (T_A=60°C). The reaction's temperature is kept at T_A for 5s to maximize the annealing efficiency. The PWM pin of VCSEL's driver is set high by Arduino to switch on the VCSEL to increase the temperature to 72°C (T_E) and hold it at T_E for 1s. After elongation stage, the UV LED irradiates the tube for 50ms. During this 50ms exposure time, Arduino collects and averages out 5 transmitted UV measurements. Since UV light is detrimental to dsDNAs, due to the crosslinking of Thymidine residues; thus, the UV exposure time is set short enough not to degrade PCR efficiency and long enough to record transmitted UV power. The transmitted power is recorded by the photodetector and displayed on Arduino's serial monitor. The photothermal heating, active cooling, and UV transmission reading are performed for 40 cycles. Using the photodetector's responsivity at 260nm, transimpedance gain, and output voltage at every cycle, the transmitted optical power is plotted against cycles.

3. RESULTS AND DISCUSSION

3.1 UV-visible spectroscopy of PCR ingredients

The contribution of each PCR ingredients to UV absorption is measured using spectrophotometer (DS-11 Series, DeNovix Inc.). Each ingredient was diluted with ddH_2O to obtain the same concentration as in positive PCR. **Figure 2** demonstrates that AuNRs and Taq are 60 to 70% percent less absorptive than 50µM dNTPs. The rest of reagents have minimal 260nm absorption.

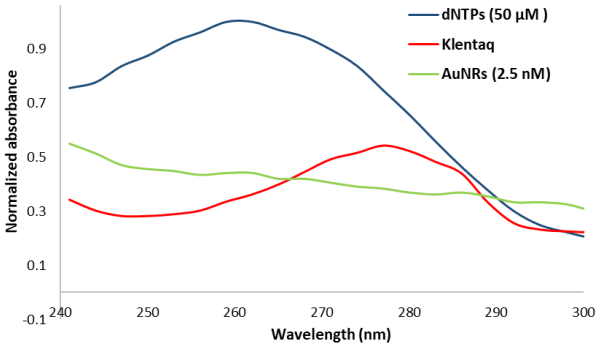

Figure 2. Comparison of UV absorption of different PCR reagents.

The reason for this can be found in high UV sensitivity of Taq polymerase due to strong UV absorption of aromatic amino acid network (tryptophan, tyrosine, and phenylalanine) present in Taq [19, 20]. Therefore, it is critical to investigate the maximum allowed UV exposure time without reducing polymerase activity. Also, prolonged UV irradiation of DNA induces formation of pyrimidine dimers which causes distortion of the DNA helix [21, 22] . This will decrease PCR efficiency, as disrupted DNA templates are less effective in subsequent PCR cycles. Therefore, the sensitivity of DNA and Taq to UV prompt us to quantify the maximum exposure time. To test this, positive PCR samples were exposed to 1mW UV LED with different time intervals from 20 to 320s. The UV exposed samples went through conventional amplification, and then the PCR products were analyzed via gel electrophoresis. The results show that UV exposure time more than 70s decreases the PCR yield significantly (**Figure 3**). Thus, the 50ms UV irradiation per cycle used in our detection strategy lies below the DNA and Taq maximum exposure time.

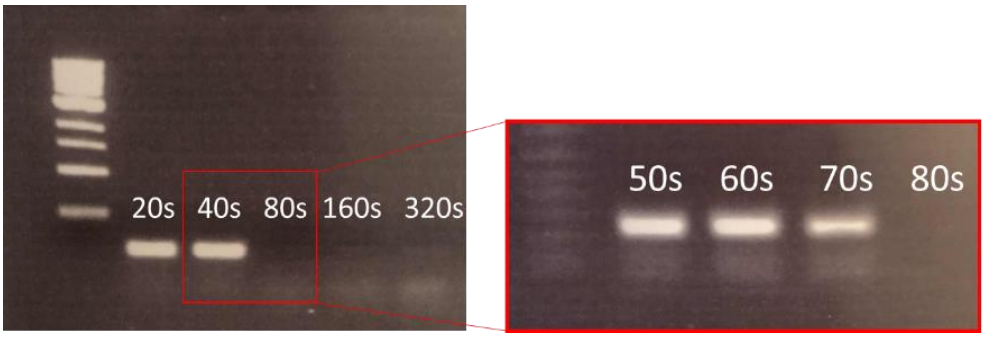

Figure 3. Different UV exposure time intervals and their impact on PCR efficiency.

3.2 VCSEL-based amplification and real-time detection

40 cycles of amplification and detection was achieved in 15mins. Here the duration of a complete PCR is extended due to the extra last ten cycles to observe the plateau phase of amplification curve. **Figure 4** shows the thermocycling curve of 20µL PCR reaction containing 10^5 copies of *Chlamydia Trachomatis* DNA compared to conventional amplification of the same sample. The gel image confirms a successful plasmonic amplification and 300bp extension of the DNA template.

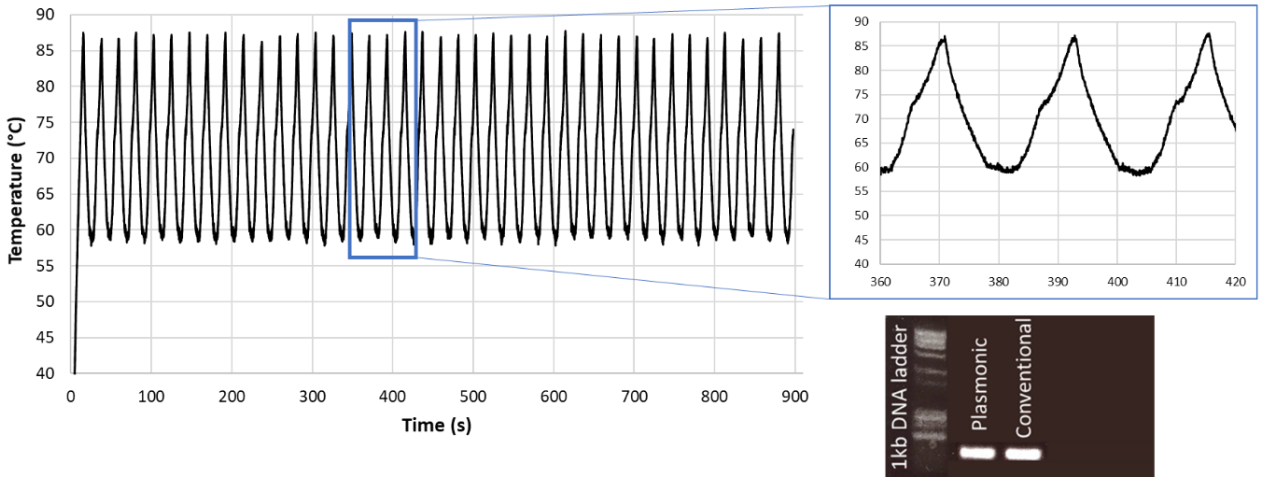

Figure 4. Demonstration of thermocycling curve, temperature stability, and comparison of plasmonic and conventional PCR products on gel electrophoresis.

The transmitted optical power was plotted versus cycles to generate the amplification curve. In fluorescent PCR, the fluorescent signal follows the PCR kinetics with a sigmoidal-shaped amplification curve. Therefore, the same behaviour is expected for the consumption of dNTPs and UV transmission signal. **Figure 5** demonstrates that the transmitted optical power (µW) imitates the amplification curve in fluorescent PCR. To highlight the phases in PCR kinetics, four different curves (second-degree polynomial, exponential, and linear) were least square fitted to original data.

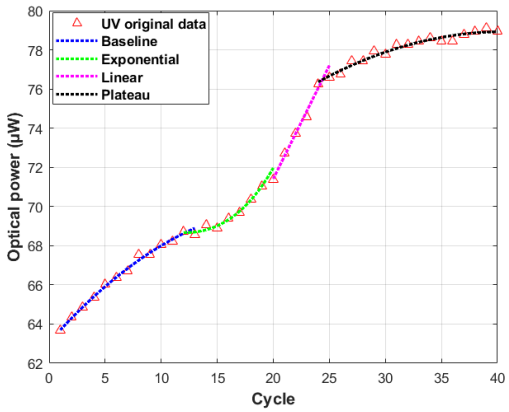

Figure 5. UV amplification curve and different curve fits to 4 phases of PCR kinetics.

3.3 Analysis of increasing baseline in UV amplification curve

We attempt to furnish a satisfactory explanation to the increasing baseline phase by plasmonic thermocycling each PCR ingredient separately. AuNRs and one reagent were diluted with ddH_2O to make 20μL sample volume, and the transmitted power was recorded for 40 cycles (**Figure 6.a**). The results indicate that only the sample containing both AuNRs and Klentaq demonstrates an increasing UV transmission whereas other ingredients have a constant or even decreasing transmission throughout 40 cycles (**Figure 6.b**). This increasing response to UV is due to greater reactivity of AuNRs towards Taq polymerase in comparison with other PCR reagents which leads to a possible change in optical properties of AuNRs [23]. Mandal et al. reported that AuNRs-Taq adduct has high thermodynamic stability and strong binding affinity which increase Taq melting temperature from 72 to 81°C, and consequently since more Taq molecules are active at normal extension temperature and above (>72°C), an increase in PCR yield was observed [23].

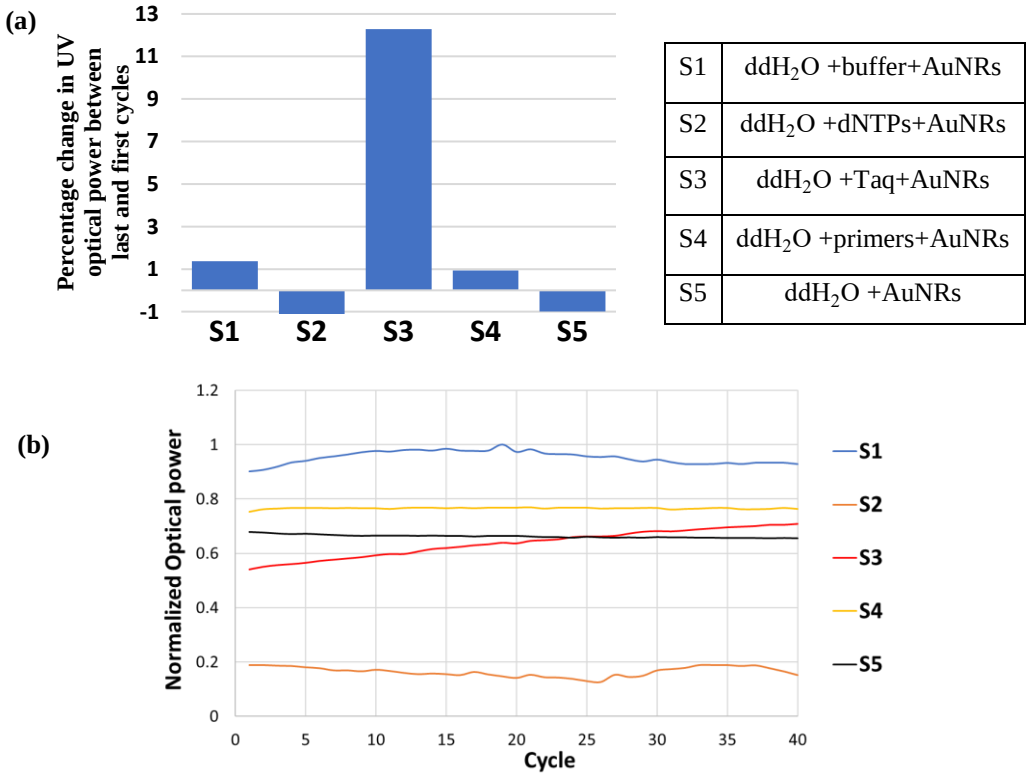

S1	ddH_2O +buffer+AuNRs
S2	ddH_2O +dNTPs+AuNRs
S3	ddH_2O +Taq+AuNRs
S4	ddH_2O +primers+AuNRs
S5	ddH_2O +AuNRs

Figure 6. (**a**) Percentage change in UV optical power for different plasmonic thermocycled reagents. (**b**) Normalized amplification curve.

3.4 PCR results classification based on shape analysis of fitted curves to UV data

The classification of PCR results (success or fail) were obtained by extracting features from the fitted curves to transmitted UV signal. Positive controls along with different negative controls were prepared and underwent plasmonic amplification and UV detection. The UV transmission for positive PCRs show a combination of a second-degree exponential curve and a sigmoidal-shaped curve which intersect at mid-cycles following a sharp increase in optical power (**Figure 7.a**). In contrast, negative controls follow a monotonically increasing second-degree exponential function which saturates after cycle 25. Therefore, the shape of amplification curve can characterize a successful and failed PCR. The bar graph in **Figure 7.b** shows the percentage increase in optical power between last and 23rd cycle ($\frac{P_{c_{40}}}{P_{C_{23}}}$) for a positive PCR is at least 7 times more than percentage increase for the same cycles in negative controls.

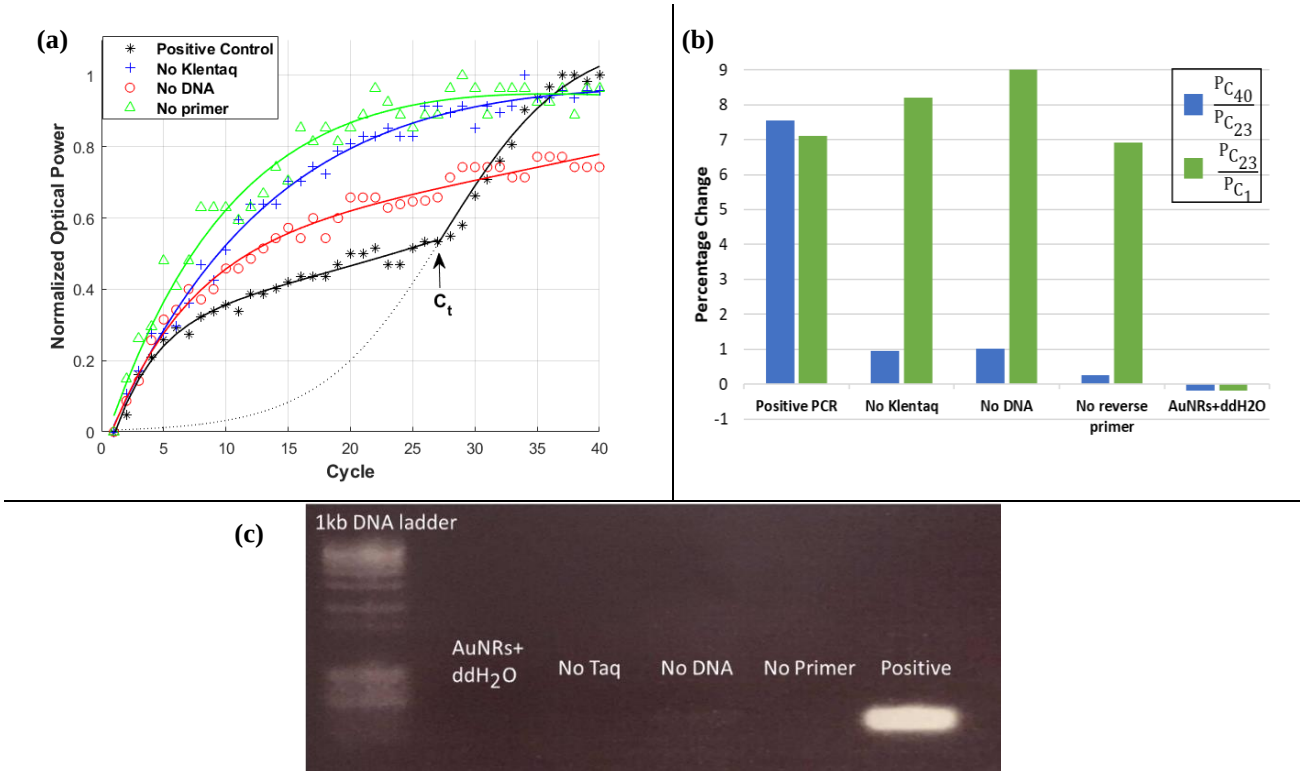

Figure 7. (**a**) Normalized amplification curve for different PCR controls. (**b**) Comparison of percentage change in UV power for different PCR controls. (**c**) PCR results on gel image.

3.5 Limit of detection

Limit of detection (LoD) is one of the most critical performance parameters in diagnostic tests. To determine LoD, PCR reactions with varying DNA template concentrations were prepared by making 10-fold serial dilutions of 10^5 DNA copies stock solution. The normalized amplification curves obtained from these reactions are shown in **Figure 8.a** and **Figure 8.b**. In fluorescent PCR, LoD is defined as the minimum DNA template concentration at which the linear phase does not appear in fluorescence curve whereas in UV monitoring, the minimum detectable amount of DNA is when the amplification curve appears as a continuous exponential curve with no sigmoidal behaviour towards the end of PCR cycles. Our real-time monitoring was able to detect abrupt increase in UV transmission close to cycle 32 for 1 DNA copy. This indicates our UV monitoring system has high sensitivity to detect PCR products generated by a single copy amplification or contaminated reagents with template. The gel image in **Figure 8.d** confirms the validity and sensitivity of UV detection assay for as small as one copy amplification.

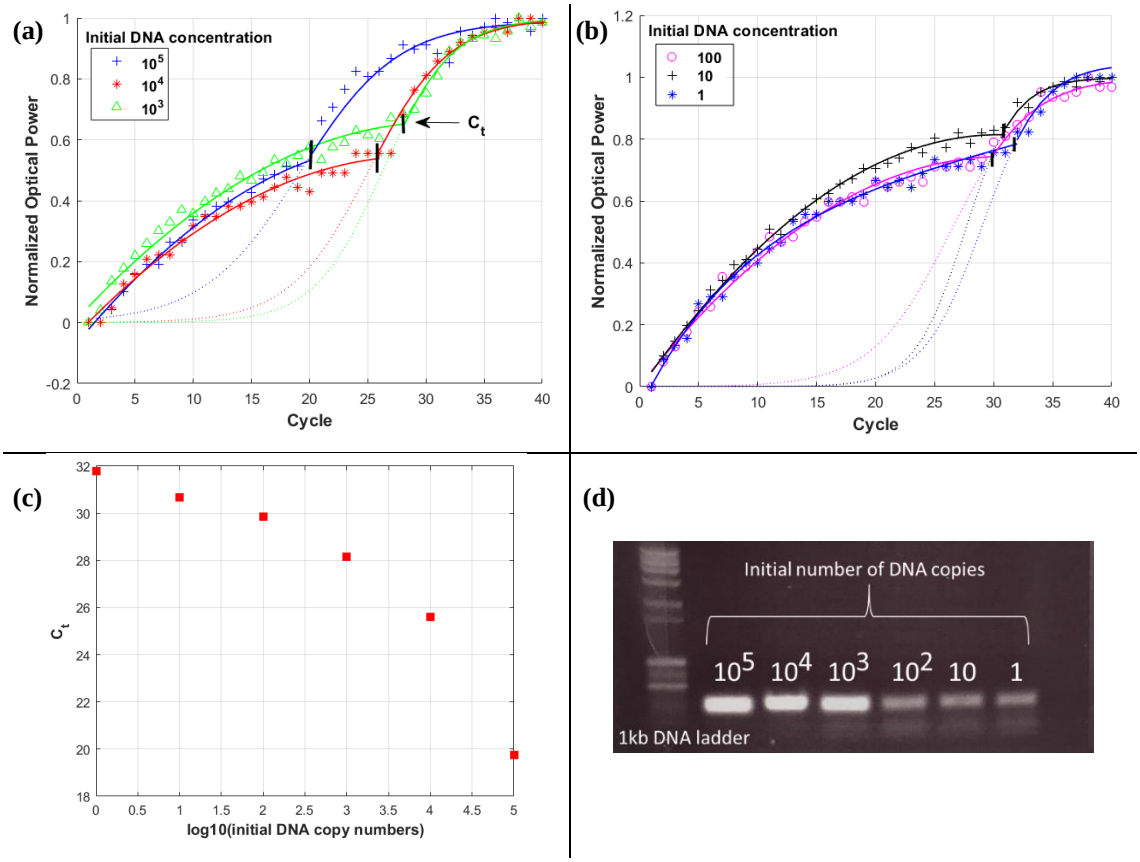

Figure 8. (**a**) and (**b**) normalized amplification curves for PCR reaction with varying DNA concentrations. (**c**) UV detection system standard curve. (**d**) Gel image of plasmonically amplified samples with different DNA concentrations.

Another way to investigate the sensitivity of the detection system is to measure the minimum detectable optical power by decreasing dNTPs' concentration. To test this, 20µL of 10mM dNTPs solution was placed in a fixed position PCR tube, and the transmitted power was recorded as the concentration was decreased by dilution factor of 2 by adding ddH_2O while maintaining the 20µL volume. The same sample preparation was repeated, but this time the absorption was measured using spectroscopy. The UV spectroscopy confirms the linear relationship between dNTPs' concentration and their absorption (**Figure 9.a** and **b**); however, this linearity saturates for concentrations more than 2.5mM and less than 5µM in our detection system, i.e, the change in concentrations more than 2.5mM and less than 5µM are not detectable (**Figure 9.c**). Consequently, exhaustion of 50µM dNTPs in PCR solution results in maximum 24% increase in detected optical power. However, during PCR this percentage increase in transmitted optical power is even less since dNTPs are converted to dsDNAs, and the newly generated dsDNAs contribute to UV absorption.

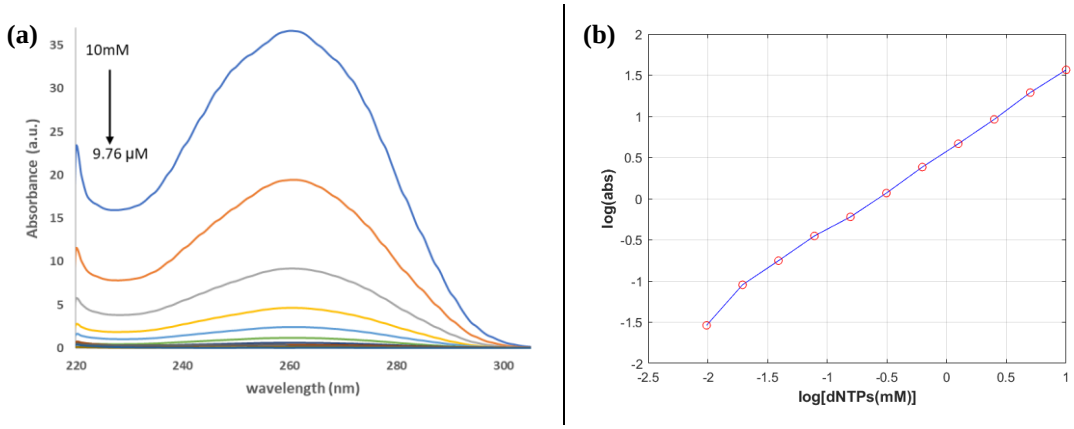

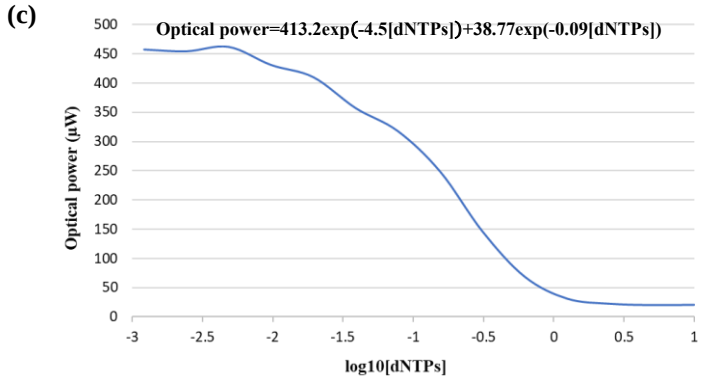

Figure 9. (**a**) UV absorption of varying dNTPs' concentrations and (**b**) linear relationship between absorption and dNTPs' concentration obtained by UV spectroscopy. (**c**) Nonlinear relationship between transmitted UV power and dNTPs' concentration.

4. CONCLUSION

We have developed a miniaturized real-time label-free PCR platform that incorporates plasmonic-driven thermocycling and UV monitoring of dNTPs exhaustion. Its compact size is derived solely from light-assisted amplification and detection and utilization of different laser type than sample miniaturization techniques. Retaining the conventional sample volume circumvents the suboptimal detection sensitivity found in fluorescent detection microfluidics due to shortened optical path length. The UV amplification curves for positive PCRs demonstrate a sigmoidal-shaped increase at C_t which can be served as a fingerprint to discriminate successful and failed PCRs. Furthermore, we presented a comparison between C_t values of positive transmission curves with different initial DNA concentrations. The result show that our detection system is capable of quantifying PCR products as small as a single DNA copy. We believe that our system has the potential to achieve more rapid cycling and more sensitive detection since factors such as optical components' configuration and alignment as well as PCR ingredients including AuNRs' concentration have not been optimized. The future work will focus on developing a multiplexed amplification and detection using VCSEL arrays and series of UV LEDs and photodetectors assembled into a handheld size box. The proposed work offers fast and reliable results in a compact, low-powered, and inexpensive hardware which makes it ideal for POC testing.

ACKNOWLEDGEMENTS

This study is supported by Génome Québec and Génome Canada (DIG-Phase 1- 9516).

REFERENCES

[1] D. Klein, "Quantification using real-time PCR technology: applications and limitations," Trends in Molecular Medicine, vol. 8, no. 6, pp. 257-260, 2002.
[2] S. Mocellin, C. R. Rossi, P. Pilati, D. Nitti, and F. M. Marincola, "Quantitative real-time PCR: a powerful ally in cancer research," Trends in molecular medicine, vol. 9, no. 5, pp. 189-95, 2003.
[3] J. Engstrom-Melnyk, P. L. Rodriguez, O. Peraud, and R. C. Hein, "Clinical Applications of Quantitative Real-Time PCR in Virology," Current and Emerging Technologies for the Diagnosis of Microbial Infections, vol. 42, pp. 161-197, 2015.
[4] Q. Phenix-Lan, S. Martin, and B. Eric, "dPCR: A Technology Review," Sensors, vol. 18, no. 4. doi: 10.3390/s18041271
[5] J. Linda and H. Johannes, "Challenging the proposed causes of the PCR plateau phase," Biomolecular Detection and Quantification, vol. 17. doi: 10.1016/j.bdq.2019.100082
[6] P. Boisseau, P. Houdy, M. Lahmani, and S. European Materials Research, Nanoscience: nanobiotechnology and nanobiology, Berlin; Springer, 2009.
[7] G. S. Makowski, Advances in clinical chemistry. Volume 40: Academic Press, 2005.
[8] J. M. Trauba and C. T. J. J. B. S. E. Wittwer, "Microfluidic extreme PCR:< 1 minute DNA amplification in a thin film disposable," vol. 10, no. 5, pp. 219-231, 2017.

[9] J. Liu, C. Hansen, and S. R. Quake, "Solving the "world-to-chip" interface problem with a microfluidic matrix," Analytical chemistry, vol. 75, no. 18, pp. 4718-23, 2003.
[10] S. Gilbert et al., "Increased sample volume and use of quantitative reverse-transcription PCR can improve prediction of liver-to-blood inoculum size in controlled human malaria infection studies," Malaria Journal, vol. 14, no. 1, pp. 1-9. doi: 10.1186/s12936-015-0541-6
[11] F. B. Myers and L. P. Lee, "Innovations in optical microfluidic technologies for point-of-care diagnostics," Lab on a chip, vol. 8, no. 12, pp. 2015-31, 2008.
[12] P. J. R. Roche et al., "Real time plasmonic qPCR: how fast is ultra-fast? 30 cycles in 54 seconds," The Analyst, vol. 142, no. 10, pp. 1746-1755, 2017.
[13] T. H. Fang et al., "Real-time PCR microfluidic devices with concurrent electrochemical detection," Biosensors and Bioelectronics, vol. 24, no. 7, pp. 2131-2136, 2009.
[14] P. Mohammadyousef, G. Uchehara, M. Trifiro, M. Paliouras, and A. G. Kirk, "Ultrafast VCSEL-based Plasmonic Polymerase Chain Reaction with Real-time Label-free Amplicon Detection for Point-Of-Care Diagnostics," in SPIE BiOS, San Francisco, California United States, 2020: SPIE International Society for Optics and Photonics.
[15] M. Tran, M. Paliouras, P. Mohammadyousef, M. Trifiro, and A. G. Kirk, "Real-time fluorophore-free optical monitoring of ultrafast DNA amplification for qPCR," presented at the 2nd European Biosensor Symposium 2019, EBS2019, Florence, Italy, 2019.
[16] H. Lodish et al., "Molecular Cell Biology, 3.0," Clinical chemistry., vol. 43, no. 4, p. 701, 1997.
[17] M. Hu and G. V. Hartland, "Heat Dissipation for Au Particles in Aqueous Solution: Relaxation Time versus Size," The journal of physical chemistry. B, Condensed matter, materials, surfaces, interfaces & biophysical., vol. 106, no. 28, p. 7029, 2002.
[18] K. Park, S. Biswas, S. Kanel, D. Nepal, and R. A. Vaia, "Engineering the Optical Properties of Gold Nanorods: Independent Tuning of Surface Plasmon Energy, Extinction Coefficient, and Scattering Cross Section," The Journal of Physical Chemistry C, vol. 118, no. 11, pp. 5918-5926, 2014.
[19] P. Kurian, A. Capolupo, T. J. A. Craddock, and G. Vitiello, "Water-mediated correlations in DNA-enzyme interactions," Physics Letters A, vol. 382, no. 1, pp. 33-43, 2018.
[20] C. Hazra, T. Samanta, and V. Mahalingam, "A resonance energy transfer approach for the selective detection of aromatic amino acids," J. Mater. Chem. C, vol. 2, no. 47, pp. 10157-10163, 2014.
[21] B. C. M. Pang and B. K. K. Cheung, "One-step generation of degraded DNA by UV irradiation," Analytical Biochemistry, Article vol. 360, no. 1, pp. 163-165, 2007.
[22] L. C. Burgess and J. O. Hall, "UV light irradiation of plastic reaction tubes inhibits PCR," BioTechniques, Article vol. 27, no. 2, pp. 252-256, 1999.
[23] S. Mandal, M. Hossain, T. Muruganandan, G. S. Kumar, and K. Chaudhuri, "Gold nanoparticles alter Taq DNA polymerase activity during polymerase chain reaction," RSC Advances, vol. 3, no. 43, pp. 20793-20799, 2013.